THE EFFECT OF A STYRENE-ACRYLIC COPOLYMER SYNTHESIZED IN A HIGH-PRESSURE REACTOR ON THE IMPROVED CORROSION PROTECTION OF A TWO-COMPONENT POLYURETHANE COATING

VPLIV STIREN-AKRILNEGA KOPOLIMERA, SINTETIZIRANEGA V VISOKOTLAČNEM REAKTORJU NA IZBOLJŠANJE KOROZIJSKE ZAŠČITE DVOKOMPONENTNEGA POLIURETANSKEGA PREMAZA

Urban Šegedin[1], Klemen Burja[2], Franci Malin[1], Saša Skale[1], Bogdan Znoj[1], Boris Šket[3], Peter Venturini[1]

[1]Central R&D of Helios Group, Helios Domžale, d. d., Količevo 2, 1230 Domžale, Slovenia
[2]Centre of Excellence for Polymeric Materials and Technologies, Tehnološki park 24, 1000 Ljubljana, Slovenia
[3]Faculty of Chemistry and Chemical Technology, University of Ljubljana, Aškerčeva 5, 1000 Ljubljana, Slovenia
urban.segedin@helios.si

In the present research the synthesis of a high-solids styrene-acrylic copolymer in a high-pressure reactor is described and a comparison of its properties with those of a copolymer synthesized at atmospheric pressure are given. The described procedure enables the synthesis of styrene-acrylic copolymers with a higher solids content under elevated pressure in a significantly shorter time, when compared to the process conducted at atmospheric pressure. The elevated pressure and higher temperature of the synthesis result in a copolymer with a lower average molecular mass and a narrower molecular mass distribution as well as a lower viscosity of the solution with an equal dry weight. Synthesized copolymers were used for the preparation of the two-component polyurethane coatings for corrosion protection. Cross-linked films were formed with a hexamethylene diisocianate homopolymer. With electrochemical impedance spectroscopy measurements a higher level of cross-linking and a lower porosity of the two-component polyurethane coating based on styrene-acrylic copolymer synthesized in a high-pressure reactor have been determined. This implies a better anti-corrosion protection of the metal substrates.

Keywords: styrene-acrylic copolymer, high-pressure synthesis, 2K-PUR coatings, electrochemical impedance spectroscopy

V raziskavi je opisan postopek sinteze stiren-akrilnega kopolimera s povečano vsebnostjo suhe snovi pri povišanem tlaku, kar vodi do skrajšanja časa sinteze v primerjavi s postopkom pri atmosferskem tlaku. Podana je primerjava lastnosti kopolimera, sintetiziranega pri povišanem tlaku, in kopolimera, sintetiziranega pri atmosferskem tlaku. Sinteza pri povišanem tlaku in višji temperaturi vodi do manjše povprečne molekulske mase, ožje porazdelitve molekulskih mas ter do nižje viskoznosti raztopine kopolimera pri enaki suhi snovi. Sintetizirana produkta sta bila uporabljena za pripravo dvokomponentnih poliuretanskih premazov za protikorozijsko zaščito. Z uporabo homopolimera heksametilen diizocianata so bili pripravljeni zamreženi premazi. Z elektrokemijsko impedančno spektroskopijo je bilo ugotovljeno, da je stopnja zamreženosti premaza s stiren-akrilnim kopolimerom, sintetiziranim pri povišanem tlaku, višja, poroznost pa nižja. To kaže na boljšo protikorozijsko zaščito kovinskih podlag.

Ključne besede: stiren-akrilni kopolimer, sinteza pri visokem tlaku, 2K-PUR premazi, elektrokemijska impedančna spektroskopija

1 INTRODUCTION

Styrene acrylic copolymers (SACs) are widely used in the coatings industry as one of the main components of coating formulations. SACs are part of one-component acrylic as well as two-component polyurethane coatings (2K-PUR). In the latter the SACs represent component A (polyol) that reacts with component B (polyisocyanate) to form polyurethane.[1] The main reaction occurs between the hydroxyl groups of the polyol and the isocyanate groups of the polyisocyanate to give urethanes. Other reactions, leading to the formation of allophanate, amine, urea, biuret and amide linkages[1–6] are shown in **Figure 1**. The amount of hydroxyl functional (meth)acrylic monomers in the SAC formulation determines the degree of cross-linking, the porosity

and the hardness of the cross-linked 2K-PUR films. When formulating the SAC, at least one hydroxyl functional (meth)acrylic monomer is used. The rest of the monomers are used to control the glass-transition temperature (T_g) and the viscosity or to give additional functionality to the SAC. Styrene is commonly used in formulations for the adjustment of T_g, hardness and the rate of physical drying. In some cases, special monomers like monoglycidyl modified esters, ethylene, propylene and alphaolefins with 7–20 carbon atoms are used to achieve higher solids and lower viscosities for the SAC solutions.[2–10]

Syntheses are usually performed at the reflux temperature of the organic solvent or the solvent mixture. The possibility of conducting reactions at elevated pressure is
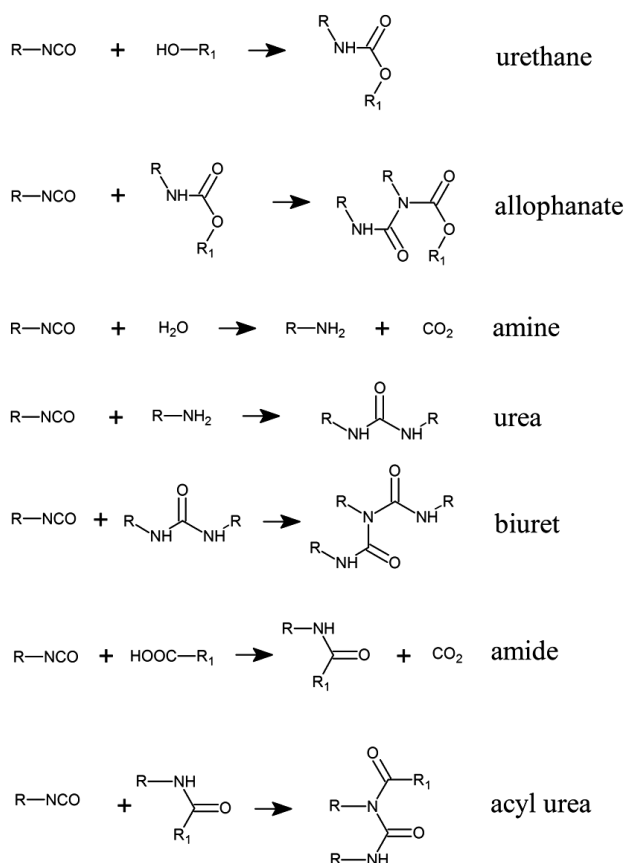
Figure 1: Formation of urethane group and other reactions present during the cross-linking of SAC and polyisocyanate[1,3]
Slika 1: Nastanek uretanske vezi ter druge reakcije pri zamreževanju SAC in poliizocianata[1,3]

mentioned in literature, but the syntheses are limited to special, highly volatile or gaseous monomers and no comparison with atmospheric-pressure synthesis has been reported.[8,9,11,12]

The effects of the process parameters on the properties of SAC are also well known.[13] The increase of the initiator concentration in the reaction mixture results in a lower average molecular mass (M_w) and faster polymerization rates. The increase in the temperature increases the polymerization rate as well. Higher reaction temperatures reduce the M_w, the molecular-mass distribution (M_w/M_n) and the viscosity.[13]

Solutions of SAC in organic solvents are being replaced by high-solids SACs (HS SACs) as a result of European legislation on volatile organic compounds (VOCs) in coatings (Directive 2004/42/CE). One way is to synthesize the SACs with a lower and less-dispersed M_w. This can be achieved by increasing the initiator concentration, slower dosing, raising the reaction temperature and using a chain-transfer reagent. In most cases the synthesis is performed in the excess solvent and distillation is needed to reach the desired dry weight. In some cases the solvent is distilled off and replaced with a more suitable solvent, and as a result lower solution viscosities are obtained.[1,2,8–13]

Electrochemical impedance spectroscopy (EIS) is a powerful tool, not only to monitor the degradation of coatings, but also a rapid non-destructive method to assess the quality of protective performance prior to the development of corrosion.[14–16] In the early stages of the coating degradation the coating's capacitance, the Warburg coefficient and the pore resistance are present. The measurements are fitted with equivalent circuits (transmission line model), which describe the charge-transfer mechanisms through the coatings (**Figure 2**). The coating capacitance (C_c) represents the water uptake in the coatings and corresponds to the charge separation on the protective film. The water accumulation on the phase boundaries between the coating and the steel substrate enables ion diffusion through the film matrix. This mechanism of charge transfer is represented by the Warburg coefficient (σ_c). Classical ion conduction through pores filled with an electrolyte solution is represented by the pore resistance (R_{po}).[14,15,17–27] EIS measurements are usually conducted in the frequency range from 10^{-2} Hz to 10^5 Hz. The results are presented as Bode and Nyquist diagrams. The high quality of 2K-PUR coatings is represented with phase values of over 80° over a wide range of frequencies and the impedance values are mainly determined by the coating's capacitance. The pure capacitor has impedance values over 10^{10} Ω cm^2, displaying superb barrier properties. With the development of pores phase and absolute impedance values decrease at lower frequencies. Typical impedance values in this case are around 10^7–10^8 Ω cm^2. The impedance values of the coatings displaying entire loss of corrosion protection are around 10^4 Ω cm^2.[16,27]

The aim of the present work is to give a comparison of the polymerization processes at atmospheric and elevated pressure. Random copolymers were synthesized via free-radical polymerization in a semi-batch process. A comparison of the properties of both end-products is presented as well. It is shown that besides a shorter reaction time the quality of cross-linked 2K-PUR films of
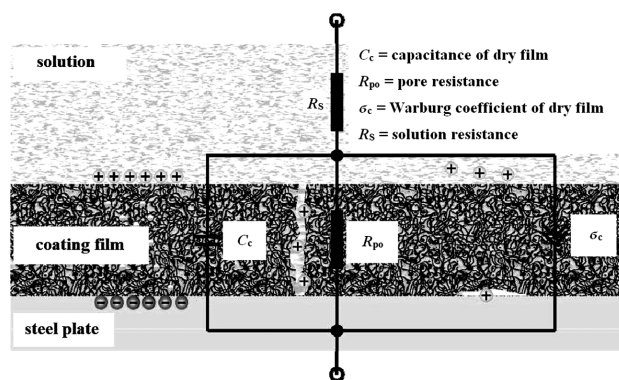

Figure 2: Charge-transfer mechanisms through the coating film during EIS measurements for the porous film prior to the development of corrosion[17]
Slika 2: Mehanizmi prenosa naboja preko premaza pri EIS-meritvah za plast z razvitimi porami pred nastankom korozije[17]

SAC synthesized in a high-pressure reactor is also improved.

2 EXPERIMENTAL

2.1 Materials

Acrylic acid (AA, Clariant), butyl acrylate (BA, BASF), 2-hydroxypropyl methacrylate (HPMA, Prochema) and styrene (S, Enichem) monomers as well as the heat-sensitive free-radical initiator t-butyl perbenzoate (t-BPB, $t_{1/2}$ = 10 h, T = 104 °C, Dow) were used for the syntheses of the SACs. Methoxypropyl acetate (MPA, BASF) served as an organic solvent. Hexamethylene diisocyanate homopolymer (HDI homopolymer; Desmodur N75 (D-N75, Bayer)) was used for the preparation of the 2K-PUR coatings.

2.2 Preparation of a monomer mixture for the syntheses of SACs

For the purpose of the present study two styrene-acrylic copolymers suitable for the preparation of the 2K-PUR coatings were synthesized. Both were prepared from the same monomer mixture containing AA, BA, HPMA and S. All the monomers were industrial grade with hydroquinone monomethyl ether (MEHQ) as a stabilizer and were used as delivered without purification. The initiator (t-BPB) was added and the mixture was stirred under mild shear conditions. The composition of the final mixture prepared for dosing is given in **Table 1**.

Table 1: Monomer mixture prepared for syntheses of SACs (mass fraction: w/%; mol fraction: x/%)
Tabela 1: Mešanica monomera, pripravljena za sintezi SAC (masni delež: w/%; molski delež: x/%)

	w/%	x/%
AA	0.8	1.31
BA	30.7	28.36
S	45.5	51.72
HPMA	21.7	17.82
t-BPB	1.3	0.79
Σ	100.0	100.00

2.3 Syntheses of SACs

Both syntheses were carried out in a semi-batch mode on a reaction calorimeter RC1e™ (Mettler Toledo) with iControl software for monitoring and controlling the process parameters.

2.3.1 The synthesis of SAC 1

SAC 1 was synthesized in a 2-L triple-wall glass reactor AP01-2-RTC with temperature sensors, calibration heater, a 4-bladed glass pitch blade stirrer, glass condenser, N₂ purge and a ReactIR 45 m Probe A with an MCT Detector using HappGenzel apodization, a DiComp (diamond) probe connected via a K6 Conduit

(16 mm probe) with a sampling area of 4000 cm⁻¹ to 650 cm⁻¹ at 8 cm⁻¹ wavelength resolution and a sampling interval of 30 s during the synthesis. Online data from FTIR (Fourier Transform Infrared Spectroscopy) measurements was collected and analyzed with iC IR software (Mettler Toledo) in real time. The reactor was filled with 400 g of MPA and heated to 135 °C at atmospheric pressure (below the boiling point of MPA at atmospheric pressure, 145 °C) with a stirring rate of 350 r/min. When the working temperature was reached, 900 g of monomer mixture with an initiator was continuously dosed into the reactor for 3 h using a Prominent Beta/4 solenoid diaphragm metering pump. After the dosing was finished the reaction mixture was kept at the working temperature for an additional 2.5 h.

2.3.2 The synthesis of SAC 2

SAC 2 was synthesized in a 1.8 L stainless-steel high-pressure reactor HP60 at a temperature of 175 °C and elevated pressure. The reactor was equipped with temperature sensors, a pressure sensor, a calibration heater, a stainless-steel anchor stirrer, a N₂ purge and an online FTIR measuring system (as described in the synthesis of SAC 1). The tightly closed reactor was filled with 300 g of MPA and 78 g of monomer mixture with an initiator and heated to 175 °C at 280 kPa of absolute pressure with a stirring rate of 200 r/min. When the working temperature was reached, 668 g of monomer mixture with an initiator was continuously dosed into the reactor for 90 min using a Prominent Beta/4 pump. After the dosing was finished the absolute pressure reached 550 kPa and the reaction mixture was kept at the working temperature for an additional 20 min, after which 15 g of the mass fraction 10 % t-BPB in MPA was dosed in 15 min for residual monomer depletion. After an additional 20 min heating at the working temperature and 570 kPa of absolute pressure the reaction mixture was cooled down and the pressure released.

2.4 Characterization of SACs

The chemical and physical properties of the products were evaluated through standard test methods. Acid-value (AV) measurements were carried out in compliance with the standard EN-ISO-2114, hydroxyl value (OH, EN-ISO-4629), dry weight of copolymer solution in MPA (DW, ISO-3251) and viscosity (η, EN-ISO-3219). The viscosity measurements were performed at 23 °C on a rotational viscometer (Haake Viscotester 550) with a coaxial cylinder sensor system.

2.4.1 Nuclear magnetic resonance (NMR) measurements

The composition of both copolymers and coatings was evaluated via ¹H and ¹³C NMR measurements. 1D ¹H and ¹³C NMR spectra of the SACs, D-N75 and 2K-PURs were recorded at 25 °C on a Unity Inova 300 MHz NMR spectrometer (Agilent Technologies). The ¹H

and ^{13}C chemical shifts were referred to the residual signal of DMSO-d6 at $\delta = 2.50 \cdot 10^{-6}$ for ^{1}H and $\delta = 39.50 \cdot 10^{-6}$ for ^{13}C.

2.4.2 Rheological properties

The rheological properties of the SAC solutions (as synthesized and diluted to the mass fraction 50 %) were assessed using a Physica MCR301 rheometer (Anton Paar GmbH). A cone-plate geometry sensor system ($R = 25$ mm, $gap = 0.207$ mm) was used to perform rotational tests where the samples were exposed to increasing shear rates (0.1 s^{-1} to 670 s^{-1}) in the first run and to decreasing shear rates (670 s^{-1} to 0.1 s^{-1}) in the second. In both cases, 29 measuring points on a logarithmic scale were taken.

2.4.3 DSC evaluations

The T_g of dried SACs was determined by differential scanning calorimetry (DSC) on a DSC 1 STAR^e System calorimeter (Mettler Toledo). The SAC samples were heated twice at 20 K/min in the temperature range from –50 °C to 200 °C with a nitrogen purge of 20 mL/min. The second heating run was used for the T_g determination. For each sample at least three distinct measurements were performed. Average values were then calculated and given as a result.

2.4.4 Gas chromatography – mass spectroscopy measurements

The amount of residual monomers in the SACs was determined with coupled gas chromatography – mass spectroscopy (GC-MS). A 6890N GC Network System with a HP-5 column with polysiloxane-based column packing (30 m in length, I. D. 0.32 mm, film 0.25 μm) and 5973 Network Mass Selective Detector (Agilent Technologies) were used. The sample solution concentration in methylenechloride was 0.1 g g^{-1} and heptane was added as an internal standard. Helium was used as an inert carrier gas with a constant flow rate of 0.7 mL min^{-1}. Standard monomer solutions with known concentrations were used for the quantitative analyses. The area under each peak was used to determine the quantity of the specific compound.

2.4.5 Size-exclusion chromatography

M_w and M_w/M_n were measured using size-exclusion chromatography (SEC) on a Waters 2690 chromatograph with a Waters 410 refractive-index detector (Waters S.A.S.). Tetrahydrofuran (THF) was used as an eluent with a flow rate of 0.7 mL min^{-1}. Three 7.8 × 300 mm single pore-sized columns with a styrene divinylbenzene copolymer column packing and a particle size of 5 μm were used in a sequence - Styragel HR 0.5 column with an effective molecular mass range of 0–10^3, Styragel HR 4E (50–10^5) and Styragel HR 5E ($2 \cdot 10^3 – 4 \cdot 10^6$). A sample solution concentration in THF was 2 mg mL^{-1}. Before the analysis the samples were filtered through a 0.45 μm PTFE filter and a 100 μL of prepared sample

was injected onto the column. As a result, the average molecular masses relative to polystyrene standards are given.

2.5 Preparation of cross-linked 2K-PUR coating films

Cross-linked 2K-PUR coating films were prepared with a HDI-homopolymer (D-N75). Diluted SAC (50 %) and D-N75 were mixed with a propeller stirrer (dry weight mass ratio 3.2 : 1) at 1500 r/min for 15 min, applied on 20 cm × 7.5 cm steel plates with an applicator and left to dry for 48 h. The dry film thickness of each 2K-PUR film was measured using the Elcometer 456 with the F1 magnetic induction probe (Elcometer Ltd.). For each film at least 20 measurements were performed, in compliance with the standard ISO 2178.

2.6 Electrochemical impedance spectroscopy

The electrochemical properties of the cross-linked coating films were measured via EIS at 20 °C. The measuring (Tait) cell for the EIS contained a working electrode (coated sample plate) with a 34.21 cm^2 area, immersed in a NaCl solution 0.1M, a hastelloy counter electrode and a standard calomel reference electrode (SCE). The potential difference between the working and the counter electrode versus SCE was -0.6 V and the amplitude of the signal was 30 mV. The measurements were performed with a Parstat 2273 Advanced Electrochemical System (Advanced Measurement Technology Inc.) and the data analyzed using the Electrochemistry Power Suite and PowerSINE software (Princeton Applied Research). The value of the frequency was in the range from 65536 Hz to 0.1 Hz.

3 RESULTS AND DISCUSSION

3.1 Syntheses of the SACs

Both syntheses described above were previously optimized in terms of dosing rate, initiator concentration and working temperature to give products suitable for the application of 2K-PUR coatings (evaluated by the amount of residual monomers in the final product, **Table 2**). The synthesis of SAC 1 was carried out at 135 °C to ensure constant conditions. The temperature for the synthesis of SAC 2 was carefully selected at 175 °C. According to the literature data, the coloration of the product progresses with temperature. In some cases 180 °C can already be too high[13]. The pressure in the synthesis of the SAC 2 was raised due to the evaporation of the solvent and the monomers as well as inflow of a fresh monomer mixture. This caused the elevation of the boiling point of the reaction mixture. Previous syntheses (not shown) indicated that an additional initiator is needed to reach a sufficient monomer conversion – a lower final residual monomer content (**Table 2**). Performing the synthesis at 175 °C significantly reduces the

reaction times in comparison to a synthesis at 135 °C (2 h 25 min versus 5 h 30 min). Higher reaction temperatures led to a lower M_w and a narrower M_w/M_n [13]. This reduces the viscosity of the system and allows for the preparation of high-solids SACs (in our case SAC 2, **Table 2**).

Table 2: Properties of synthesized SACs
Tabela 2: Lastnosti sintetiziranih SAC

	SAC 1	SAC 2
DW [w/%]	62.4	71.3
η/(mPa s) (23 °C, 0.1 s^{-1})	8200	15500
M_w	23000	9000
M_w/M_n *	2.6	2.3
T_g/°C **	32 ± 2	23 ± 2
AV [mg KOH / g dry copolymer]	9.3	9.3
OH [mg KOH / g dry copolymer]	110	110
Residual monomers [w/%]	0.5	0.4

* ratio between mass average (M_w) and number average molecular mass (M_n)
** $T_{g, Fox}$ = 33.3 °C

Figure 3 shows a comparison of both syntheses through thermal conversion. The reaction calorimeter measured the heat released due to the polymerization (q_r) in real time. From this data the thermal conversion was calculated as the ratio between the heat release until a certain time (t_r) and the total heat release from the reaction (t_{tot} stands for the total reaction time):

$$X_{th} = \frac{\int_0^{t_r} q_r(t)\mathrm{d}t}{\int_0^{t_{tot}} q_r(t)\mathrm{d}t} \qquad (1)$$

It should be stressed that a 100 % thermal conversion does not imply total monomer consumption. For a better
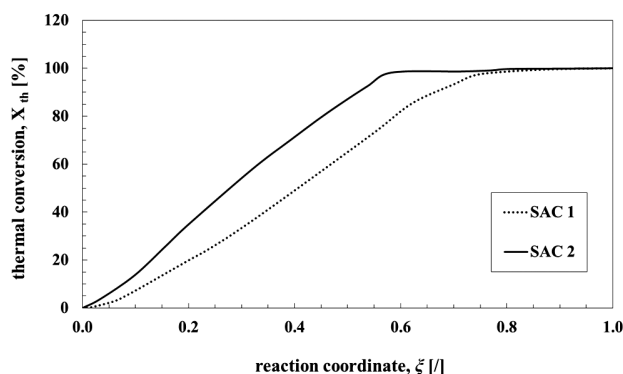

Figure 3: Thermal conversion for polymerizations of SACs
Slika 3: Termična konverzija pri polimerizacijah SAC

comparison the x-axis in **Figure 3** is not absolute time, but rather the reaction coordinate (ξ), defined as the progress of syntheses ($\xi = 0$ meaning start of dosing, $\xi = 1$ meaning the end of synthesis – the beginning of cooling the reaction mixture down). **Figure 3** shows that in the synthesis of SAC 2, a 98.2 % thermal conversion was reached after the dosing was completed (at $\xi = 0.56$), whereas in the synthesis of SAC 1 only a 74.4 % thermal conversion was achieved (at $\xi = 0.58$). In terms of heat removal, only 1.8 % of all the reaction heat needed to be removed after the dosing in the synthesis of SAC 2. On the other hand, in the synthesis of SAC 1, 25.6 % of all the reaction heat needed to be removed after the dosing was completed. In terms of heat release controlled by dosing, the synthesis in a high-pressure reactor turns out to be safer than the synthesis at a temperature below the boiling point of the solvent.

3.2 Characterization of the SACs

The described syntheses performed on the RC1e™ reaction calorimeter were made in parallel. There were no discrepancies between the parallels in terms of
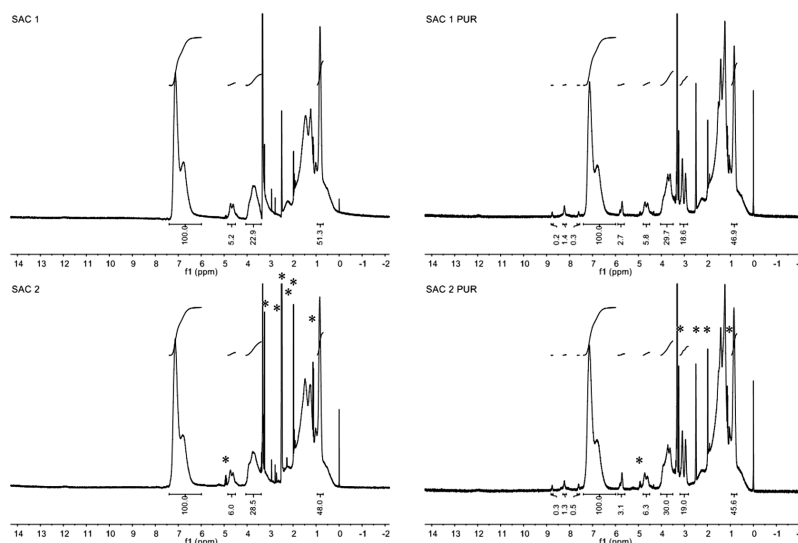

Figure 4: Comparison of ^{1}H NMR spectra of SACs and 2K-PURs; * denotes signals of solvents MPA and DMSO at 2.5 · 10^{-6}
Slika 4: Primerjava ^{1}H-spektrov SAC in 2K-PUR; * označuje signale topil MPA in DMSO pri 2,5 · 10^{-6}

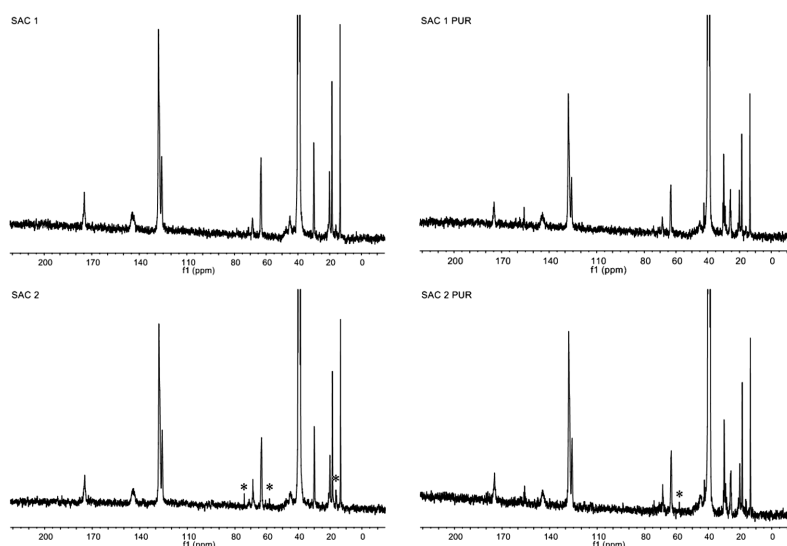**Figure 5:** Comparison of ^{13}C NMR spectra of SACs and 2K-PURs; * denotes signals of solvent MPA
Slika 5: Primerjava ^{13}C-spektrov SAC in 2K-PUR; * označuje signale topila MPA

process parameters due to the excellent process control. Therefore, the syntheses were highly reproducible. This resulted in matching properties of the products such as M_w, M_w/M_n, residual monomers and viscosity. The results are not shown due to the negligible differences.

Furthermore, analyses of the acid and hydroxyl values (**Table 2**) confirmed the same functionality of both SACs. Since the on-line FTIR data provided insufficient information on the SACs' composition, NMR measurements were performed. The ^{1}H and ^{13}C NMR spectra of the dry SACs and 2K-PURs show no significant differences in functionality. As can be seen in **Figure 4** there are no peaks in the $5–6 \cdot 10^{-6}$ range of the ^{1}H NMR spectra of the SACs that are assigned to the protons around the double bonds of the (meth)acrylic monomers. Also, there is no peak at $112 \cdot 10^{-6}$ in the ^{13}C NMR spectra of the SACs assigned to vinyl =CH$_2$ of styrene (**Figure 5**). This supports the GC-MS measurements of the residual monomers and implies that the monomer mixture was sufficiently converted to the copolymer.

The HDI homopolymer ^{1}H NMR spectrum (**Figure 6**) shows peaks at $8.3 \cdot 10^{-6}$ (-NH-CO-, biuret H), $3–3.5 \cdot 10^{-6}$ (-CH$_2$-N=, HDI) and $1–2 \cdot 10^{-6}$ (-CH$_2$-, HDI). The typical peaks in the ^{13}C NMR spectrum are at $155 \cdot 10^{-6}$ (-NH-CO-N, biuret), $121 \cdot 10^{-6}$ (-NCO, isocyanate) and $25–45 \cdot 10^{-6}$ (-CH$_2$-, HDI). This confirms the structure of the HDI homopolymer (D-N75). The HDI monomers react with water to form trimers with a biuret linkage. These trimers further react to form the HDI-homopolymer.

In the preparation of the 2K-PURs the depletion of the –NCO group in the ^{13}C NMR spectra can be seen (**Figure 5**, SAC 1 PUR and SAC 2 PUR), whereas the peaks at 8.3 (^{1}H NMR) and $155 \cdot 10^{-6}$ (^{13}C NMR) assigned to the biuret remain visible. The urethane

groups are overlapping with the styrene aromatic ring ($7 \cdot 10^{-6}$ and $7–7.8 \cdot 10^{-6}$ in ^{1}H NMR spectra, **Figure 4**). Small amounts of urea produced by side reactions can be seen from the ^{1}H NMR spectra at $5.7 \cdot 10^{-6}$ [28–31]. The
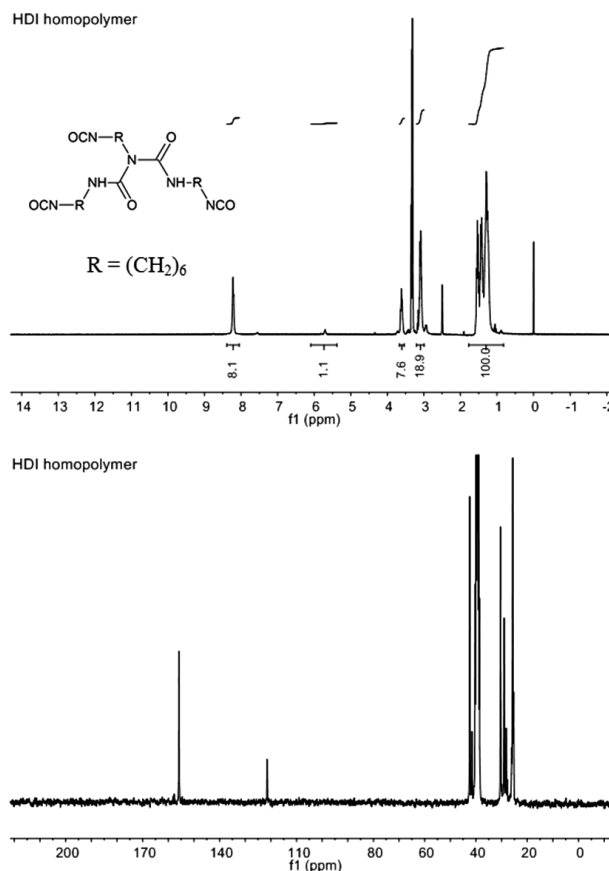

Figure 6: ^{1}H and ^{13}C NMR spectra of HDI homopolymer with trimer structure
Slika 6: ^{1}H- in ^{13}C NMR-spektra HDI homopolimera s strukturo trimera
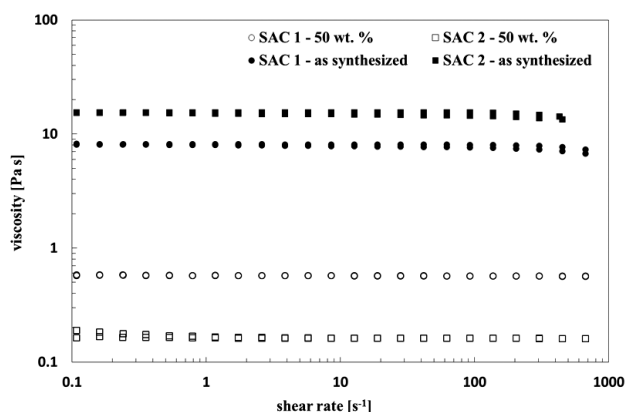
Figure 7: Flow curves of original (closed symbol) and diluted SACs (open symbol)
Slika 7: Tokovne krivulje osnovnih (črne oznake) in razredčenih SAC (bele oznake)

NMR results show the similar composition of both SACs and of both 2K-PUR films.

As **Table 2** shows, a high solids SAC was synthesized (DW of SAC 2 > 70 %). A higher temperature in the synthesis of the SAC 2 led to a lower M_w (9000 versus 23000) and a narrower M_w/M_n (2.3 versus 2.6). The shorter copolymer chains result in a decrease of the SAC 2 T_g in comparison to the SAC 1 (23 °C versus 32
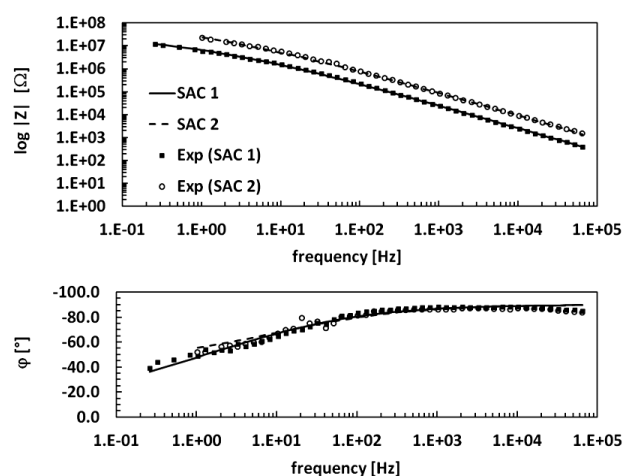
°C), which complies with the literature data[13]. Both SACs have a T_g lower than that predicted by the Fox equation (33 °C). The viscosity of the SAC 2 is higher due to the higher solids content (15500 mPa s versus 8200 mPa s, **Table 2**, **Figure 7**). After the dilution of both SACs with additional solvent to 50 % the effect of shorter copolymer chains can be observed as lower viscosity values (160 mPa s versus 570 mPa s, **Figure 7**). Both products were suitable for the preparation of 2K-PUR coatings.

The results of the EIS measurements and the evaluations for cross-linked 2K-PUR films of SAC 1 and SAC 2 are shown in **Figure 8** (Bode diagrams) and **Figure 9** (Nyquist diagram) and the fitting model parameters are given in **Table 3**. The experimental data were fitted by equivalent circuits – the transmission-line model[16,19,27] – indicating a better quality of cross-linked 2K-PUR film prepared with the SAC 2. The transmission-line model for the SAC 2 film has no pore resistance ($R_{po} > 10^9$ Ω cm^{-2}, **Figure 9**), indicating that no pores are developed. The lower Warburg coefficient (σ_c) of the SAC 2 represents a better cross-linking of the shorter SAC chains and a lower coating capacitance (C_c) represents a lower water uptake of the cross-linked 2K-PUR film prepared with the SAC 2 in comparison to the one prepared with SAC 1.[12,16,17,27] The impedance values shown in the Bode and Nyquist diagrams (**Figures 8** and **9**) for cross-linked 2K-PUR films prepared with the SAC 1 and SAC 2 in combination with comparable film thicknesses (**Table 3**) of both films directly indicate the better quality of the SAC 2.[16,17,27] The impedance values at low frequencies are above 10^7 Ω for both films and the improved quality of the 2K-PUR film prepared with the SAC 2 can be seen. The generally accepted absolute value of the impedance for the
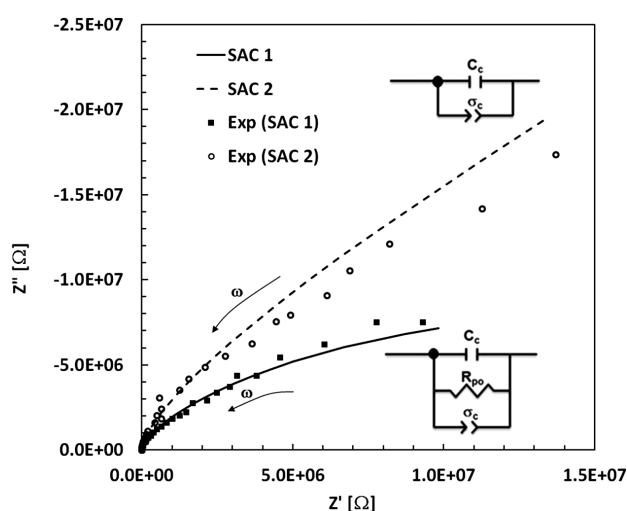

Figure 8: Bode diagrams for cross-linked 2K-PUR films; lines represent the fitting model
Slika 8: Bodejeva diagrama za zamrežene 2K-PUR premaze; črte prikazujejo prileganje modela

Table 3: Electrochemical properties of cross-linked 2K-PUR films
Tabela 3: Elektrokemijske lastnosti zamreženih 2K-PUR premazov

	SAC 1	SAC 2
d_c/μm	75 ± 3	65 ± 3
σ_c/(Ω^{-1} rad$^{-1/2}$ s$^{1/2}$ cm^2)	4.2×10^{-8}	1.3×10^{-8}
R_{po}/(Ω cm^{-2})	3.7×10^7	ND
C_c/(F cm^{-2})	6.1×10^{-9}	1.7×10^{-9}
d_c = thickness of cross-linked 2K-PUR film σ_c = Warburg coefficient of film R_{po} = pore resistance C_c = capacitance of cross-linked 2K-PUR film		

Figure 9: Nyquist diagram for cross-linked 2K-PUR films (SAC 1 and SAC 2) with equivalent circuits used for fitting model (R_S not shown); ω arrow denotes the increase in angular frequency
Slika 9: Nyquistov diagram zamreženih 2K-PUR premazov (SAC 1 in SAC 2) z odgovarjajočima nadomestnima tokokrogoma (R_S ni prikazan); ω puščica kaže v smeri naraščanja kotne frekvence

protective coatings is at least 10^6 Ω.[32] This means that both SACs are suitable for the preparation of 2K-PUR coatings.

4 CONCLUSIONS

Synthesis in a high-pressure reactor under high temperature and elevated pressure proved to be a better alternative to the synthesis of high-solids SACs in a solution of an organic solvent at atmospheric pressure. The proposed direct synthesis leads to a product with no need of subsequent solvent removal by distillation and compliant with the European legislation on volatile organic compounds in coatings. Apart from the significant cutoff in the reaction times a much higher thermal conversion is reached while the monomer mixture is still being dosed when compared to the synthesis below the reflux temperature of the solvent. The cross-linked 2K-PUR coating prepared with the SAC 2 shows better anti-corrosion properties in comparison to the SAC 1, making it suitable for the protection of metal substrates.

Acknowledgements

5 REFERENCES

[1] D. K. Chattopadhyay, K. V. S. N. Raju, Progress in Polymer Science, 32 (**2007**), 352–418
[2] U. Poth, R. Schwalm, M. Schwartz, Acrylic Resins, Vincentz Network, Hannover 2011
[3] J. Huybrechts, P. Bruylants, A. Vaes, A. De Marre, Progress in Organic Coatings, 38 (**2000**), 67–77
[4] D. E. Fiori, Progress in Organic Coatings, 32 (**1997**), 65–71
[5] Z. W. Wicks Jr., D. A. Wicks, J. W. Rosthauser, Progress in Organic Coatings, 44 (**2002**), 161–183
[6] M. Melchiors, M. Sonntag, C. Kobusch, E. Jürgens, Progress in Organic Coatings, 40 (**2000**), 99–109
[7] A. Kumar, R. K. Gupta, Fundamentals of polymer engineering, second edition, Marcell Dekker Inc., New York 2003
[8] A. I. Yezrielev, M. G. Romanelli, W. E. Welman, Improved high solids acrylic based coatings, EPA 0 225 809 A2, 1987
[9] G. W. Meyer, J. E. M. Fletcher, High solids acrylic resin, WO 02/066527, 2002
[10] W. J. Blank, High solids polymer resin coating composition containing amino resin cross-linking agent, GB 2 112 398 A, 1982
[11] C. J. Bouboulis, Superior solvent blends for synthesis of acrylic resins for high solids coatings, EP 0 099 647 B1, 1983
[12] M. Manea, High Solid Binders, Vincentz Network, Hannover 2008
[13] M. Slincxs, N. Henry, A. Krebs, G. Uytterhoeven, Progress in Organic Coatings, 38 (**2000**), 163–173
[14] J. N. Murray, Progress in Organic Coatings, 31 (**1997**), 375–391
[15] S. Skale, V. Doleček, M. Slemnik, Progress in Organic Coatings, 62 (**2008**), 387–392
[16] Y. Zhu, J. Xiong, Y. Tang, Y. Zuo, Progress in Organic Coatings, 69 (**2010**), 7–11
[17] S. Skale, Evaluation of Epoxy Coatings Surface Protection with Electrochemical Impedance Spectroscopy, Doctoral Dissertation, University of Maribor, Faculty of Chemistry and Chemical Engineering, Maribor, 2009
[18] M. G. Fontana, Corrosion Engineering, 3rd Ed., McGraw-Hill Book Company, New York 1986
[19] S. Skale, V. Doleček, M. Slemnik, Corrosion Science, 49 (**2007**), 1045–1055
[20] D. D. Macdonald, Techniques for Characterization of Electrodes and Electrochemical Processes, John Wiley & Sons, Inc., New York 1991, Ch. 11
[21] F. Mansfeld, Journal of Applied Electrochemistry, 25 (**1995**), 187–202
[22] M. Kendig, J. Scully, Corrosion, 46 (**1990**), 22–29
[23] A. S. Castela, A. M. Simoes, Corrosion Science, 45 (**2003**), 1631–1646
[24] B. Liu, Y. Li, H. Lin, C. N. Cao, Corrosion, 59 (**2003**), 817–820
[25] M. Stratmann, Corrosion, 61 (**2005**), 1115–1124
[26] T. Skoulikidis, A. Ragoussis, Corrosion, 48 (**1992**), 666–670
[27] R. Posner, K. Wapner, S. Amthor, K. J. Roschmann, G. Grundmeier, Corrosion Science, 52 (**2010**), 37–44
[28] B. S. Selukar, S. P. Parwe, K. K. Mohite, B. Garnaik, Advanced Materials Letters, 3 (**2012**), 161–171
[29] E. Žagar, M. Žigon, Polymer, 40 (**1999**), 2727–2735
[30] E. Žagar, M. Žigon, Polymer, 41 (**2000**), 3513–3521
[31] Y. Kaya, M. Kamaci, Polimery, 56 (**2011**), 721–733
[32] J. R. Vilche, E. C. Bucharsky, Corrosion Science, 44 (**2002**), 1287–1309